Chapter 6

Purification, Rheological Characterization, and Visualization of Viscous, Neutral, Hetero-exopolysaccharide Produced by Lactic Acid Bacteria

S. Ikeda, D. Kondoh, N. P. D. Aryantini, T. Urashima, and K. Fukuda

Abstract

Viscous exopolysaccharide (EPS)-producing lactic acid bacteria (LAB) have received increasing interest in the dairy industry because of their capability to improve the texture and mouthfeel of fermented dairy products. To date, enormous efforts have been made to reveal the relationship between texture and EPS production in fermented milk products such as yogurt. However, the structure-rheology relationship of EPSs themselves is not yet well understood due to their low yields in general and their wide variety of chemical structures. In this chapter, we describe common techniques for the purification, visualization, and rheological analysis of viscous EPSs produced by LAB.

Key words Atomic force microscopy, Dynamic viscoelasticity, Light microscopy, Transmission electron microscopy, Negative staining

1 Introduction

Some lactic acid bacteria (LAB) produce exopolysaccharides (EPSs), which can be divided into two different types: homo-EPS consisting of a single sugar residue such as dextran, a polymer of glucose, and hetero-EPS, which is a polymer of repeating units of various sugar residues [1]. In general, the former has a relatively simple structure and high production yields compared to the latter, owing to the attributes of their biosynthetic pathways. Several homo-EPSs have already been commercialized, but progress is hindered to some extent for hetero-EPS produced by LAB, mainly due to their low production yields (ranging from a few to hundreds of milligrams), with a few exceptions [1]. Despite the technical setbacks, studying the relationship between chemical structures and physicochemical properties of hetero-EPSs produced by LAB is important for their industrial application. Furthermore, such knowledge would be useful in interpreting the reported health

Makoto Kanauchi (ed.), *Lactic Acid Bacteria: Methods and Protocols*, Methods in Molecular Biology, vol. 1887,
https://doi.org/10.1007/978-1-4939-8907-2_6,

benefits of hetero-EPSs from LAB, such as antitumor [2], blood cholesterol-lowering [3], and immunomodulating [4] properties, in view of the structure-function relationships.

Lactobacillus fermentum MTCC 25067 (formerly TDS030603) was previously isolated from Indian fermented milk, *dahi*, as a good producer of viscous EPSs. This strain secretes approximately 100 mg of slime hetero-EPS in 1 L of de Man-Rogosa-Sharpe broth when it grows statically at 30 °C for 24 h under aerobic conditions [5]. The resulting 1% EPS solution is highly viscous, exhibiting an apparent viscosity of 0.88 Pa·s at a shear rate of 10 s^{-1}, which was comparable to the viscosity of xanthan gum, a commercial viscosity modifier produced by *Xanthomonas campestris*.

In this chapter, we introduce how to visualize and analyze the physicochemical properties of viscous, neutral, hetero-EPSs using an EPS from *L. fermentum* MTCC 25067 as a typical example. First, procedures to obtain thoroughly purified EPS are summarized. Next, to clarify the physicochemical properties of the EPS, dynamic viscoelasticity measurements were performed. Finally, to obtain data that support the interpretation of physicochemical properties of the EPS, visualization techniques, including light microscopy, transmission electron microscopy, and atomic force electron microscopy, were introduced. For further information on analytical procedures of chemical structures of homo- and hetero-EPS, *see* Chapter 7 by Gerwig GJ.

2 Materials

2.1 Purification

1. Ice-cold ethanol.
2. 50 mM Tris–HCl buffer (pH 8.7). Store at 4 °C.
3. DEAE-Sephadex A-50 for anion-exchange chromatography.
4. Toyopearl HW-55F for gel filtration.
5. Spectra/Por 1 dialysis tubing, MWCO 6000–8000.

2.2 Rheological Characterization

1. Mineral oil.
2. A cone and plate geometry attachment with a cone radius of 20 mm and a cone angle of 1°.
3. A concentric cylinder geometry attachment with a cup radius of 15 mm, a bob radius of 14 mm, and a bob height of 42 mm.
4. An HR-2 Discovery Hybrid rheometer.

2.3 Visualization

2.3.1 Light Microscopy

1. 70% ethanol.
2. Gram's crystal violet solution.
3. 20% (w/v) copper sulfate.
4. Immersion oil.
5. Microscope slides (76 × 26 × 0.9–1.2 mm).
6. Cover glasses (22 × 22 mm).
7. Disposable inoculating loops.
8. BX53 upright microscope with 100× objective lens.

2.3.2 Transmission Electron Microscopy

1. 0.1 M phosphate buffer (pH 7.4).
2. 2.5% glutaraldehyde in phosphate buffer.
3. 1% OsO_4 in phosphate buffer.
4. Ethanol series (70%, 80%, 90%, 95%, and 100% ethanol).
5. LR white resin.
6. Ultramicrotome.
7. Diamond knives (Sumi knife 45° and Sumi knife XAC).
8. Copper grids of 150 mesh.
9. Transmission electron microscope HT7700.
10. 4% uranium acetate.

2.3.3 Atomic Force Microscopy

1. Muscovite mica grade V-1 in 25 mm × 75 mm sheets.
2. Stainless steel mounting discs, 15 mm in diameter.
3. Cyanoacrylate glue.
4. Scotch tape.
5. V-shaped silicon nitride cantilever probes of a nominal spring constant of 0.4 N/m and a resonant frequency of 70 kHz.
6. A BioScope Catalyst atomic force microscope mounted onto an inverted optical microscope.

3 Methods

3.1 Purification

1. Dilute 1 L of the cultured broth with four volumes of ion exchange water (IEW) (*see* **Note 1**), and centrifuge at 10,000 × *g*, 4 °C for 30 min. Collect supernatant by decantation, add an equal volume of ice-cold ethanol to the diluted supernatant, and keep at 4 °C overnight. Centrifuge the mixture at 17,000 × *g*, 4 °C for 30 min, discard supernatant, add 100 mL of 50 mM Tris–HCl (pH 8.7) to the pellet, and transfer the suspension to 50-mL conical tubes. Dissolve the pellet by vigorous shaking at 4 °C overnight.

2. Add a 200-mL slurry of DEAE-Sephadex A-50 equilibrated with 50 mM Tris–HCl (pH 8.7) to the EPS solution and mix very well (*see* **Note 2**). Remove the resin on the glass filter by aspiration. Lyophilize the EPS solution.
3. Add 100 mL of IEW to the lyophilized EPS and dissolve thoroughly by vigorous shaking (*see* **Note 3**). Apply the EPS solution to a Toyopearl HW-55F column (2.6 × 100 cm, 15 mL/h) equilibrated with IEW. Collect the EPS fractions, concentrate to approximately 10 mL by rotary evaporation, dialyze against milli-Q water overnight at 4 °C overnight (*see* **Note 4**), and lyophilize. Keep the lyophilized EPS in a desiccator.

3.2 Rheological Characterization

3.2.1 Steady Shear Viscosity Measurement

1. Dissolve EPS in IEW to 0.01–2% (w/w), heat the solutions at 80 °C for at least 10 min, and cool them to ambient temperature (*see* **Note 5**).
2. Pour 25 mL of a 0.01–0.2% (w/w) EPS solution into the cup attachment preset at 25 °C, or place 40 μL of a 0.3–2.0% (w/w) EPS solution on the plate attachment preset at 25 °C, lower the upper part of the attachment to a preset gap, and cover the sample solution surface with mineral oil to prevent the evaporation of water (*see* **Note 6**).
3. Measure steady shear viscosity at 25 °C in a shear rate range from 0.1 to 100 s^{-1} (*see* **Note 7**). By plotting steady shear viscosity values as a function of shear rate on a double-logarithmic scale, one should see a plateau at low shear rates. The plateau value of steady shear viscosity represents the zero-shear viscosity of the sample solution (Fig. 1a).
4. Plot zero-shear viscosity values as a function of EPS concentration. One should see gradual increases in viscosity at relatively low EPS concentrations and steeper increases at higher EPS concentrations due to more enhanced entanglements between molecular chains of EPS (Fig. 1b). The zero-shear viscosity of various polysaccharide solutions plotted against concentration on a double-logarithmic scale increases linearly with increasing concentration, while the slope increases from 1.3–1.4 to 3.3–5.1 at a critical concentration at which individual molecules are brought into contact with one another [6, 7].

3.2.2 Dynamic Viscoelasticity Measurement

1. Immediately following steady shear viscosity measurement, the sample solution is subjected to a dynamic viscoelasticity measurement. Measure the strain dependence of storage modulus (G') and loss modulus (G'') at a constant temperature of 25 °C, a constant frequency of 1 Hz, and strains progressively increased from 0.001–0.2 to ensure that both moduli are independent of strain around a strain of 0.01 (*see* **Note 8**).

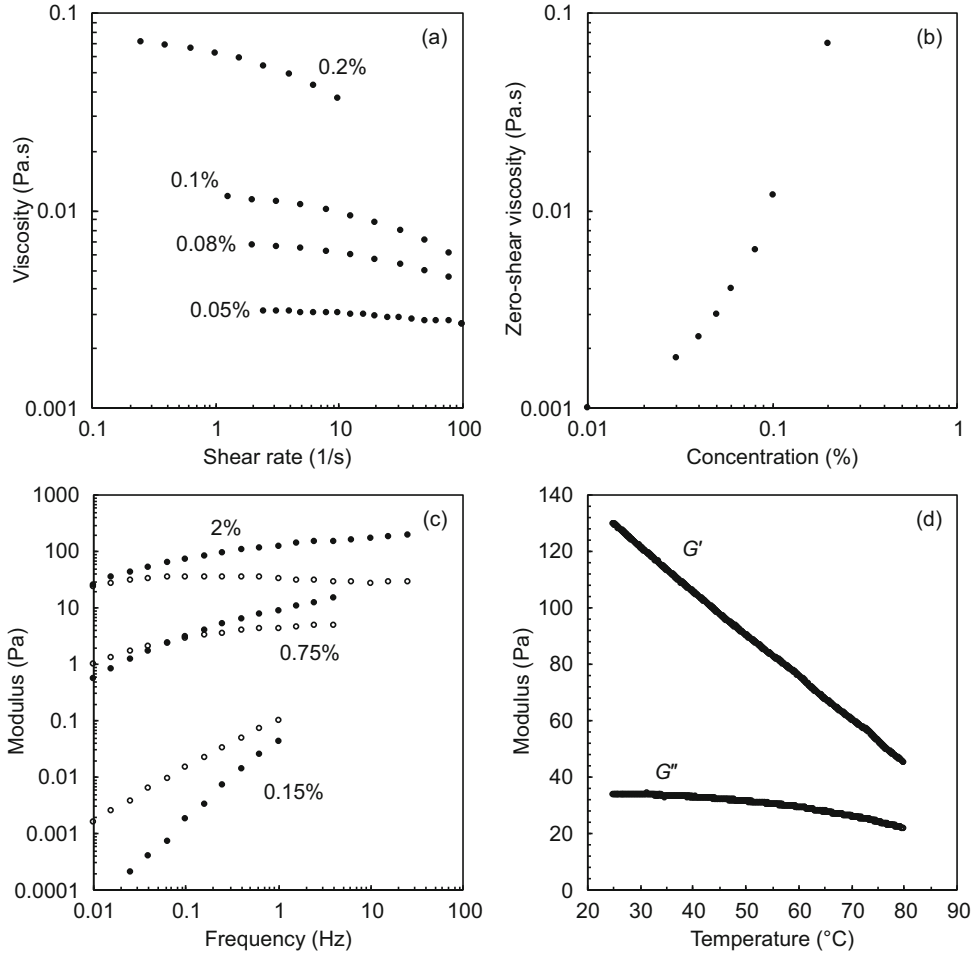

Fig. 1 Rheological characterization of a neutral hetero-EPS produced by *L. fermentum* MTCC 25067. (**a**) Shear rate dependence of steady shear viscosity. (**b**) Concentration dependence of zero-shear viscosity. (**c**) Frequency dependence of storage modulus (filled) and loss modulus (open). (**d**) Temperature dependence of the storage modulus (G') and loss modulus (G'') of a 2% EPS solution

2. Measure the frequency dependence of G' and G'' at a constant temperature of 25 °C, a constant strain of 0.01, and frequencies progressively increased from 0.01–100 Hz (*see* **Note 9**). Figure 1c illustrates the frequency dependence of the moduli of a typical EPS solution. EPS solutions show $G' < G''$ at low frequencies with G' being more frequency dependent. As the frequency is increased, there is a crossover between G' and G''. The crossover frequency is considered to be inversely related to the relaxation time of entangled molecular chains [7–9], and hence decreases with increasing EPS concentration (*see* **Note 10**).
3. Heat the sample solution to 80 °C and measure the temperature dependence of G' and G'' at a constant strain of 0.01, a

constant frequency of 1 Hz, and temperatures progressively decreased from 80–25 °C at a rate of −1 °C/min. Both G' and G'' should increase monotonically with decreasing temperature without any abrupt changes (Fig. 1d) (*see* **Note 11**).

3.3 Visualization

3.3.1 Light Microscopy

1. Clean all the slide, and cover glasses with 70% ethanol. Place a single drop of crystal violet solution at the edge of a microscope slide.
2. Aseptically transfer and suspend a single colony thoroughly in the crystal violet solution on the slide.
3. Spread the bacterial suspension gently on a new microscope slide, and air-dry (*see* **Note 12**).
4. Wash with 20% copper sulfate solution and air-dry (*see* **Note 13**).
5. Observe under a light microscope with 100x objective lens covered with immersion oil (Fig. 2a) (*see* **Note 14**).

3.3.2 Transmission Electron Microscopy

1. Fix colonies of viscous neutral hetero-EPS producing LAB on agar by applying 2.5% glutaraldehyde in phosphate buffer for 2 h (*see* **Note 15**).
2. After discarding the fixative, wash the colonies three times with phosphate buffer on the plate.
3. Transfer phosphate buffer containing some colonies into a 1.5-mL tube using a cut-tip pipette, discard the buffer, and then postfix the specimens by applying 1% OsO_4 in phosphate buffer for 30 min.
4. After discarding the fixative, wash postfixed colonies three times with phosphate buffer.
5. Dehydrate the specimens through an increasing concentration of ethanol series (70%, 80%, 90%, 95%, and two times with 100%).
6. After discarding the 100% ethanol, apply LR white resin in the tube for 2 h.
7. Transfer the colonies into gelatin capsules containing new LR white resin using a cut-tip pipette. Keep it at room temperature for 1 h, and then polymerize the resin at 60 °C overnight.
8. Cut an ultrathin section (90 nm in thickness) of the colonies using an ultramicrotome and a diamond knife. Place the section on a copper grid, and dry it out.
9. Prepare a drop of 4% uranium acetate on parafilm, and put the section side of the grid on this drop for 1 min (*see* **Note 16**). Next, wash the grid with distilled water, and dry it out.
10. Observe the ultrathin section using an H7700 transmission electron microscope (80 kV) (Fig. 2b).

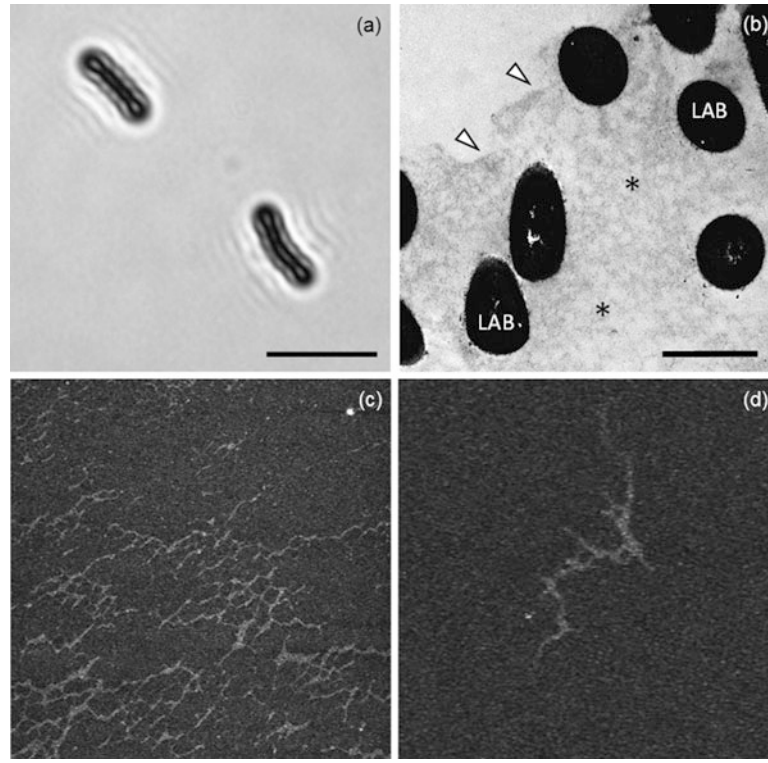

Fig. 2 Visualization of a neutral hetero-EPS produced by *L. fermentum* MTCC 25067. (**a**) Negative staining of the EPS with crystal violet. Bar = 10 μm. (**b**) Transmission electron microscopic image of the EPS (*). Arrowheads indicate the end of the colony. Bar = 1 μm. (**c**) Topographical AFM image of the EPS deposited from a 1 ppm solution. The image size is 3 μm × 3 μm. (**d**) Topographical AFM image of the EPS deposited from a 0.1 ppm solution. The image size is 1 μm × 1 μm

3.3.3 Atomic Force Microscopy

1. Dissolve EPS in milli-Q water to 0.1–1 μg/mL (*see* **Note 17**).
2. Cut a mica sheet of 10 mm × 10 mm using scissors. Place 10 μL of the cyanoacrylate glue in the center of a steel mounting disk and the mica sheet onto it, press gently, and let the glue dry.
3. Cleave the mica surface using Scotch tape. Deposit 2 μL of the sample solution onto the freshly cleaved mica surface, and let it dry until no liquid is visible. Place the completed mounting disk in the microscope stage and clamp it.
4. Mount a probe onto the cantilever holder and the cantilever holder into the AFM head. Align the laser on the cantilever to give a sum signal of at least 6 V. Adjust the position of the laser spot in the photodetector to a vertical position of −2 V and a horizontal position of 0 V (*see* **Note 18**).

5. Mount the AFM head onto the microscope stage for imaging in air using ScanAsyst mode. Set the scan size to 500 nm, the scan rate to 1 Hz, and the scan angle to 0 degrees. Turn on ScanAsyst auto control, and engage the probe to the mica surface. After the engagement, set the scan size to 3–5 μm and the scan rate to 0.5–1 Hz to obtain a low-resolution overview (Fig. 2c). Decrease the scan size to 1–2 μm, and set the scan rate to 1 Hz to obtain a higher-resolution image (Fig. 2d) (*see* **Note 19**).

4 Notes

1. Dilution is not necessary when the viscosity of the cultured media is not so high that it interferes with pelleting bacterial cells by centrifugation.
2. Anion-exchange chromatography is not necessary when the protein concentration of the crude EPS solution is negligible. When the viscosity of the EPS solution is not so high, column separation is an alternative. For acidic EPS, column chromatography should be used.
3. Thorough solubilization of EPS may take several days depending on its water solubility.
4. Thorough desalting is critical to achieve highly pure EPS. More than 400 volumes of milli-Q water rather than of EPS solution should be used in dialysis, and it is better to change milli-Q water to a fresh solution several times.
5. For measuring the steady shear viscosity of a less viscous EPS, increase concentrations as necessary. Heating EPS solutions at an elevated temperature helps to hydrate EPS.
6. The concentric cylinder attachment has a much larger area of contact with a sample solution and provides greater sensitivity and hence should be used whenever a sufficient volume (ca. 25 mL) of an EPS solution is available.
7. The signal-to-noise ratio tends to be low at low shear rates, particularly at low EPS concentrations. The lowest shear rate at which viscosity can be practically determined increases with decreasing EPS concentration. At high shear rates, apparent shear thickening (i.e., an increase in viscosity with increasing shear rate) may be observed. This is an indication of the occurrence of turbulent flow accompanied by more enhanced viscous dissipation of kinetic energy.
8. Dynamic viscoelasticity measurements must be performed using small strains within the linear viscoelastic region, where both G' and G'' are independent of strain. The range of strain within the linear viscoelastic region may extend up to 0.1 or

10%. A strain of 0.01 is reasonably large, while a larger strain gives a better signal-to-noise ratio.

9. Similar to the case of steady shear viscosity measurement, the signal-to-noise ratio tends to be low at low frequencies, particularly at low EPS concentrations. The lowest frequency at which G' and G'' can be practically determined increases with decreasing EPS concentration. Measurements at high frequencies are also limited due to difficulties in correcting the inertia of moving parts of the rheometer as well as the inertial response of the sample solution [10].
10. These rheological characteristics of EPS solutions should be distinguished from those of true gels that show $G' > G''$ and almost frequency-independent moduli throughout the experimentally accessible frequency range due to their extremely long relaxation times and hence extremely small crossover frequencies [9].
11. Polysaccharides that form thermo-reversible gels upon cooling show steep increases in the moduli in a relatively narrow temperature range due to the conformational transition of the polysaccharide molecules and gradual increases outside the narrow temperature range [9, 11, 12]. Gradual increases in the moduli in the entire temperature range confirm that the EPS does not form a thermos-reversible gel at the examined EPS concentration and temperatures.
12. Thermal drying should be avoided to ensure the EPS remains intact and to prevent bacterial cells from shrinking, which may result in the formation of a clear zone surrounding the cells.
13. Washing with water may cause a loss of EPS.
14. Crystal violet stains both the bacterial cell wall and acidic EPS. However, it could be washed out with 20% copper sulfate solution from neutral EPS, resulting in the formation of a halo.
15. At this time, most colonies are detached from the agar.
16. The application of uranium acetate is recommended to render viscous neutral hetero-EPS, although transmission electron microscopic images of LAB themselves are obtained even without this process.
17. EPS may concentrate in small areas on the mica surface during air-drying, making it difficult to locate it. In such a case, increase the concentration to 2–10 μg/mL. A drawback of increasing the concentration is that it may impede the visualization of individual molecules [13, 14]. It is possible, however, that EPS needs to be deposited from an even higher concentration solution in the case that EPS does not dissociate into individual molecules during hydration and remains as supramolecular assemblies [15].

18. If the force exerted by the probe becomes too high, the sample may deform, be displaced, or even be dissected. If this turns out to be the case, increase the vertical position of the laser spot in the photodetector to up to 0 V.
19. The vertical resolution of AFM is ca. 0.1 nm [16], while the thickness of a polysaccharide chain in an AFM image can be 10 or more times higher than its measured height [17, 18]. This is known as the probe tip broadening effect where the degree of broadening depends on the geometry of the probe tip [19]. Care must be taken when comparing the thicknesses of EPS molecular chains from AFM images and those from electron microscopy images.

Acknowledgments

We are grateful to Prof. Richard W. Hartel and Dr. Hassan Firoozmand at the University of Wisconsin-Madison for their technical assistance with the rheological analyses.

References

1. Zeidan AA, Poulsen VK, Janzen T, Buldo P, Derkx PMF, Øregaard G, Neves AR (2017) Polysaccharide production by lactic acid bacteria: from genes to industrial applications. FEMS Microbiol Rev 41(Supp_1):S168–S200
2. Wang K, Li W, Rui X, Chen X, Jiang M, Dong M (2014) Characterization of a novel exopolysaccharide with antitumor activity from *Lactobacillus plantarum* 70810. Int J Biol Macromol 63:133–139
3. Maeda H, Zhu X, Omura K, Suzuki S, Kitamura S (2004) Effects of an exopolysaccharide (kefiran) on lipids, blood pressure, blood glucose, and constipation. Biofactors 22:197–200
4. Chabot S, Yu HL, de Leseleuc L, Cloutier D, Van Calsteren MR, Roy D, Lacroix M, Oth D (2001) Exopolysaccharides from *Lactobacillus rhamnosus* RW-9595M stimulate TNF, IL-6 and IL-12 in human and mouse cultured immunocompetent cells, and IFN-γ in mouse splenocytes. Lait 81:683–698
5. Fukuda K, Shi T, Nagami K, Leo F, Nakamura T, Yasuda K, Senda A, Motoshima H, Urashima T (2010) Effects of carbohydrate source on physicochemical properties of the exopolysaccharide produced by *Lactobacillus fermentum* TDS030603 in a chemically defined medium. Carbohydr Polym 79:1040–1045
6. Morrs ER, Cutler AN, Ross-Murphy SB, Rees DA, Price J (1981) Concentration and shear rate dependence of viscosity in random coil polysaccharide solutions. Carbohydr Polym 1:5–21
7. Robinson G, Ross-Murphy SB, Morris ER (1982) Viscosity-molecular weight relationships, intrinsic chain flexibility, and dynamic solution properties of guar galactomannan. Carbohydr Res 107:17–32
8. Cuvelier G, Launay B (1986) Concentration regimes in xanthan gum solutions deduced from flow and viscoelastic properties. Carbohydr Polym 6:321–333
9. Ikeda S, Nishinari K (2001) "Weak gel"-type rheological properties of aqueous dispersions of nonaggregated κ-carrageenan helices. J Agric Food Chem 49:4436–4441
10. Atakhorrami M, Koenderink GH, Schmidt CF, MacKintosh FC (2005) Short-time inertial response of viscoelastic fluids: observation of vortex propagation. Phys Rev Lett 95:208–302
11. Ikeda S, Nitta Y, Temsiripong T, Pongsawatmanit R, Nishinari K (2004) Atomic force microscopy studies on cation-induced network formation of gellan. Food Hydrocoll 18:727–735

12. Funami T, Hiroe M, Noda S, Asai I, Ikeda S, Nishinari K (2007) Influence of molecular structure imaged with atomic force microscopy on the rheological behavior of carrageenan aqueous systems in the presence or absence of cations. Food Hydrocoll 21:617–629
13. Ikeda S, Nitta Y, Kim BS, Temsiripong T, Pongsawatmanit R, Nishinari K (2004) Single-phase mixed gels of xyloglucan and gellan. Food Hydrocoll 18:669–675
14. Ikeda S, Gohtani S, Nishinari K, Zhong Q (2012) Single molecules and networks of xanthan gum probed by atomic force microscopy. Food Sci Technol Res 18:741–745
15. Ikeda S, Shishido Y (2005) Atomic force microscopy studies on heat-induced gelation of curdlan. J Agric Food Chem 53:786–791
16. Heymann JB, Möller C, Müller DJ (2002) Sampling effects influence heights measured with atomic force microscopy. J Microsc 207:43–51
17. Ikeda S, Gohtani S, Nishinari K, Zhong Q (2013) High acyl gellan networks probed by rheology and atomic force microscopy. Food Sci Technol Res 19:201–210
18. Ikeda S, Henry K (2016) Effects of partial replacement of gelatin in high sugar gels with gellan on their textural, rheological, and thermal properties. Food Biophys 11:400–409
19. Ivanov YD, Frantsuzov PA, Bykov VA, Besedin SP, Hoa GHB, Archakov AI (2010) Comparative investigation of PdR by usual and ultrafine atomic force microscopy. Anal Methods 2:688–693